NUMERICAL ANALYSIS OF THE 10 BAR MASCOTTE FLOW FIELD

Mani POUROUCHOTTAMANE[♦], Francis DUPOIRIEUX[♦],
Lucien VINGERT[♦], Mohammed HABIBALLAH[♦], and
Victor BURNLEY[§]
[♦]ONERA - B.P. 72 – 92322 CHATILLON CEDEX – France
[§]Air Force Research Laboratory, visiting scientist at ONERA

1. Introduction

In liquid propulsion area, as in many other fields, aspects like reliability, delays and cost reduction become a priority. The use of calibrated design tools (CFD codes) may help to make the primary design choice associated to reliable and reduced cost technologies. As far as delays are concerned, they can be reduced by using improved and calibrated predicting tools since the latter will allow to limit the total number of qualifying tests and to focus on the identified critical operational range of a combustion device for instance. CFD analysis may be also used to help directing development tests, analyzing test results and consequently helps to reduce costs and delays.

As far as the propulsion system is concerned, Oxygen/Hydrogen engines are usually the most preferred, due to their high performance. Although the technology of such engines is well known, physical-chemical processes involved in their operation are not all well described yet. In particular, the combustion chamber flow dynamics still arises many questions, in the scientific community. In order to get insight into the complex phenomena involved in the operation of such engines, a research programme has been carried out for several years, in the framework of the GDR research group, involving CNRS, ONERA, SNECMA Moteurs and CNES. The objective of this programme is to step forward in the understanding of the physical-chemical processes taking place in cryogenic (LOX/GH_2) rocket engine combustion chambers, and to build up appropriate modelling of such processes. The ultimate goal of such an approach is to provide calibrated predictive CFD tools that can be used during the development programme of launcher propulsion systems.

In the framework of the GDR, ONERA has developed a cryogenic test facility, called Mascotte[1-3], to improve the understanding and modelling of the elementary processes involved in LOX/GH_2 combustion. The facility was designed and built up from 1991 to 1993, in the ONERA Palaiseau center, and has been operating since 1994. A large database is now available for model and code validation.

In parallel to the research programme, workshops on Rocket Combustion Modelling (RCM) are organized in cooperation with Germany in the framework of the French-German Memorandum of Understanding on high pressure combustion. The objectives of such workshops is to assess the capabilities of CFD codes to predict liquid rocket engine like flows. To this end, documented test cases are proposed to the contributors.

The first workshop was held in Toulouse (France) in 1998 and the second one in Heilbronn (Germany) in 2001. This paper is a contribution to this second workshop. It deals with the test case RCM2 which consists in the numerical simulation of the 10 bar Mascotte flow field. The test case was computed using the ONERA MSD code. In the following sections, characteristics of the MSD code, computational geometry, injection conditions and models used are first described. Then, results are compared with experimental data and discussed.

2. The MSD code

The MSD code solves the unsteady, three-dimensional, Reynolds-Averaged, Navier-Stokes equations, for a mixture of perfect gases. Discretization is based on finite volume techniques on curvilinear structured grids. The time integration can be either explicit, then a predictor-corrector scheme is used, or implicit with first or second-order accuracy. The implicit algorithm uses a classical ADI factorisation. The spatial discretization scheme is second-order accurate. The Euler fluxes are evaluated through a "Flux Difference Splitting" TVD scheme. The viscous fluxes are calculated at the center of cells and then interpolated on the cell interfaces.

The code presents many features like multi-domain integration; fast convergence towards steady-state solutions can be achieved through multigrid cycles. $k-\varepsilon$ type two-equation models, with Boussinesq closure or ASM closure, are available for the treatment of turbulence and several combustion models are implemented in this code (purely kinetical models and turbulent combustion models).

A Lagrangian solver, named DLS, is also available for particle tracking with one-way or two-way coupling with the gas phase.

3. The Mascotte combustor and computational geometry

The Mascotte combustor and geometry are those specified for the test case RCM2. There are depicted in figures 1 and 2.

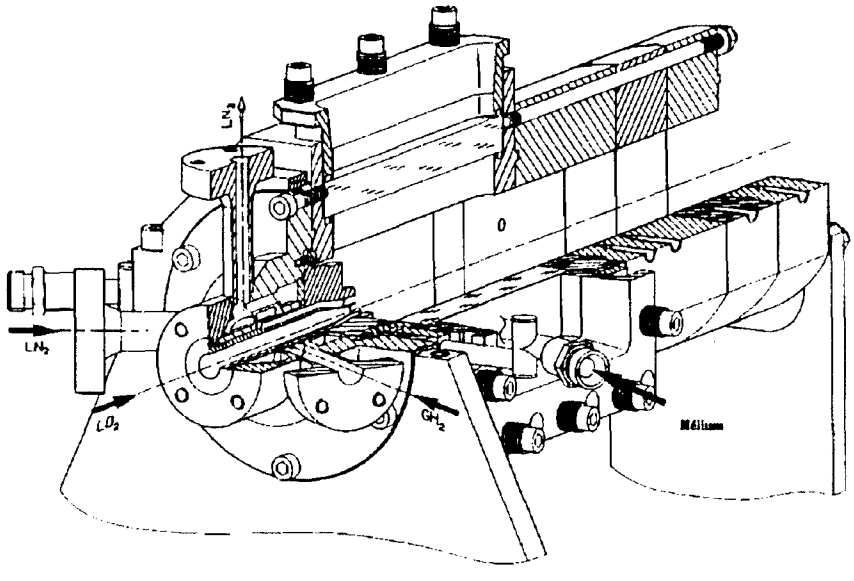

Figure 1: Mascotte Combustor

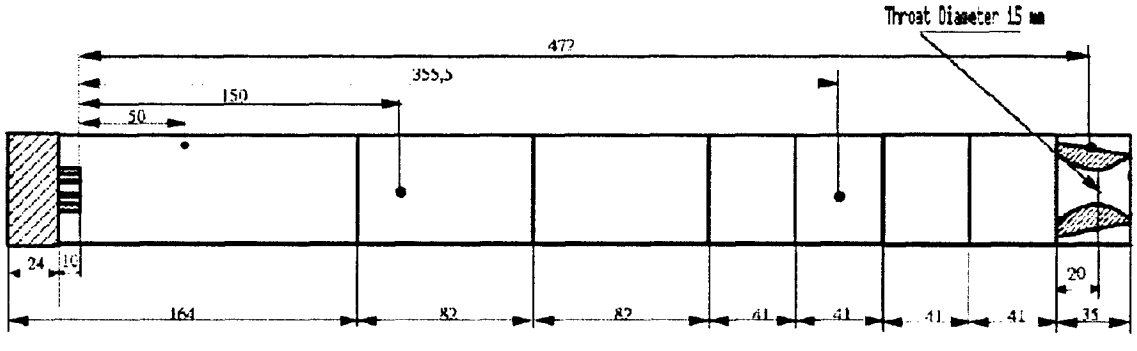

Figure 2: Combustor geometry (in mm) for the 10 bar case

Simulation were performed using a simplified injector geometry given below :

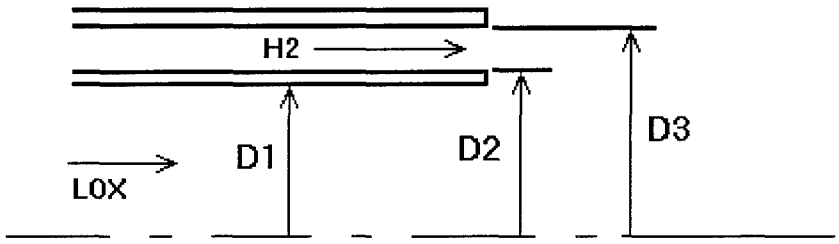

	D1	D2	D3
DIAMETER	5.0 mm	5.6 mm	12.0 mm

Numerical simulations were carried out either with a 2D (axisymmetrical geometry) or a 3D (slice of 5° with one cell in the tangential direction) geometry (Fig. 3). The oxygen liquid core is represented by a solid cone (Fig. 4) which length is 7.8 mm. The length *Lc* was determined using the following correlation[4]:

$$\frac{L_C}{D_1} = \frac{6}{\sqrt{J}}$$

D_1 being the inner LOX post diameter and J the hydrogen to oxygen momentum flux ratio. Droplets are injected along the cone. Although the chamber is square, we assumed an axisymmetrical geometry, presuming that the phenomena take place mainly in the centrepart of the chamber, therefore neglecting the boundary effects.

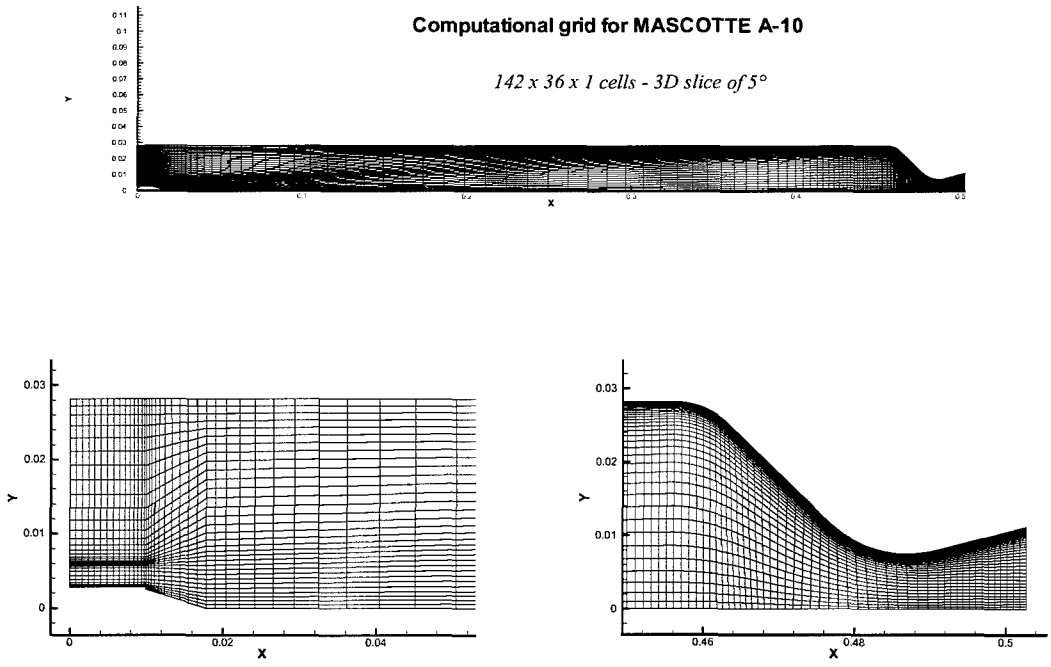

Figure 3: Computational geometry and grid

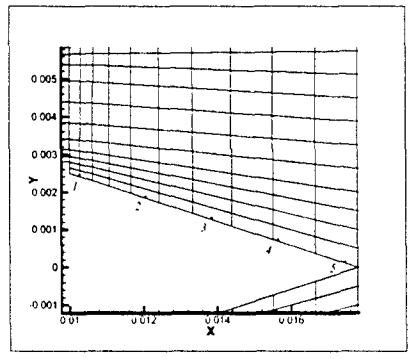

Figure 4: Liquid core representation and injection points

4. Operating point and injection conditions

The operation point is A-10 which characteristics are :

PRESSURE	O/F	$\dot{m}$ (LOX)	$\dot{m}$ (H2)
10 bar	2.11	50 g/s	23.7 g/s

Hydrogen is injected gaseous at 287 K. Oxygen is supposed to be atomized and droplets are injected along the core in five locations as shown in figure 4. The injection velocity is 10 m/s and the direction of velocity is given by an empirical correlation[5] :

$$\theta(x) = \arctan[R_i(1 - x/L_c)/(x + R_i/\tan\theta_i)]$$

where $\theta_i = \theta(0)$, $\tan\theta_i = 0.68(U_{gas}/U_{liq} - 1)\sqrt{\rho_{gas}/\rho_{liq}}$,

$R_i = D_1/2$, L_c is the core length and x is the axial distance from the injector exit to the point of injection. Only one class of diameter has been considered.

To investigate the effect of the injection diameter, some computations were performed using three values of the diameter : 50 µm, 82 µm, 115 µm. In fact, flow visualisation showed that the atomisation process is very complex and far from being complete (presence of ligaments) in the near exit region. Nevertheless, some atomisation data could be obtained by means of a one-component PDPA (Phase Doppler Particle Analyzer) at 30 mm from the injector with an acceptable validation rate (47%). These measurements represent the droplet data at the closest location from the injector exit and could be used as inlet boundary condition. The diameter 115 µm corresponds to the Sauter mean diameter given by the PDPA at that location. 82 µm, which was the recommended value, is the Sauter mean diameter of the same distribution truncated at 250 µm by removing a small number of big droplets, and 50 µm was chosen for comparison.

5. Physical modelling

The two-phase turbulent reactive flow generated in the single-element Mascotte combustor is computed using the classical Eulerian-Lagrangian Method. Reynolds Averaged Navier-Stokes equations are solved for the gas and droplets are tracked using the Lagrangian solver DLS. A two-way coupling is performed between the liquid phase and the gas phase. Gas phase turbulence is computed with the $k-\varepsilon$ turbulence model. The turbulent dispersion is treated by the Gossman and Ionnides Eddy Life Time dispersion model with an additional spatial decorrelation criterion[6] to better account for crossing trajectory effect. Vaporization is computed with the standard "D^2" model with Ranz-Marshall correction to account for convection around the droplet. Four combustion models were used for these computations : two kinetic models (the Rogers and Chinitz model and

the Eklund model) and two turbulent models (the Magnussen's Eddy break-up model and the CLE model). Although experimental data including OH imaging and Coherent Anti-Stokes Raman Scattering (CARS) indicated a highly turbulent flame, kinetic combustion models were used for comparison. The CLE turbulent combustion model assumes an infinitely fast single scalar chemistry with a β-function pdf and a thermodynamical equilibrium limitation[7].

6. Results

Figure 5 shows radial temperature profile obtained with the two kinetic models at 200 mm from the injector exit. One can notice that both models predict a longer flame than expected and a still stratified temperature field at this location.

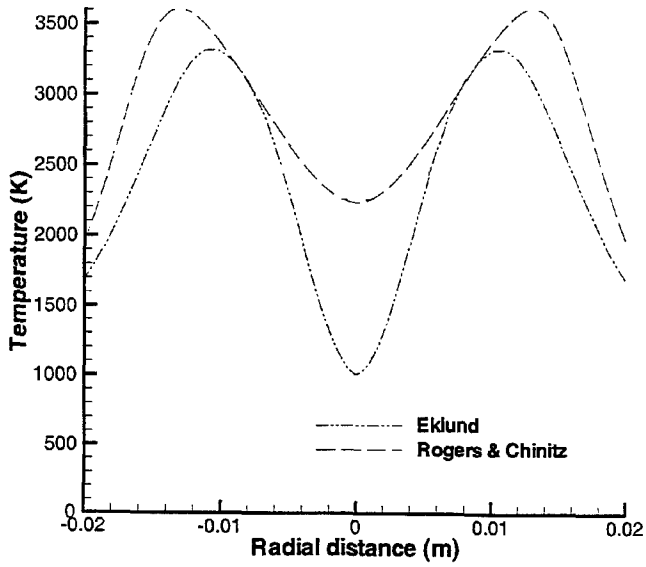

Figure 5 : Temperature profiles (x = 200 mm) – Kinetic models

Computations were also performed using the turbulent combustion models : the Magnussen model and the CLE model. Figure 6 shows a comparison of temperature field for both models. The flame shapes are similar but the Magnussen model gives a very high flame temperature (4500 K). This is due to the single step reaction used in the model that includes only three species O_2, H_2, and H_2O. Dissociation of these molecules into radicals (in particular OH) is ignored leading to an overestimation of the flame temperature.

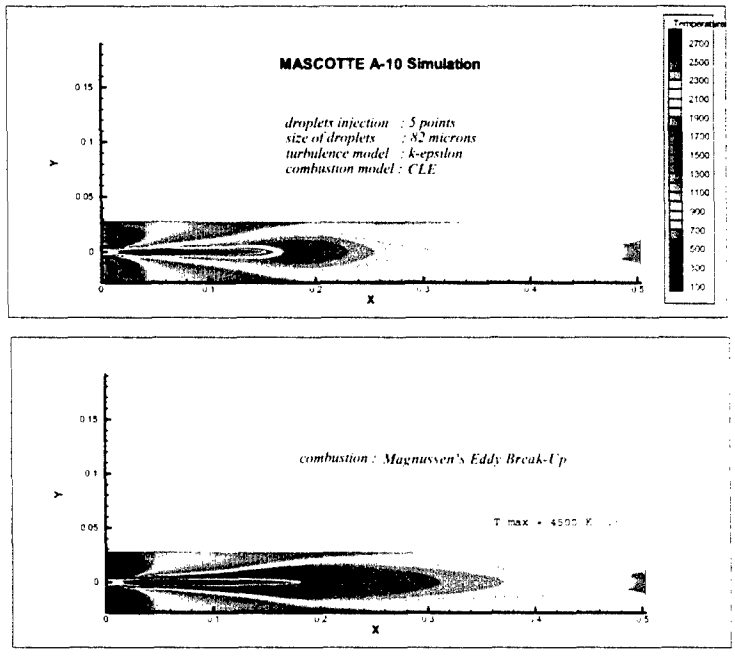

Figure 6 : Temperature field – The Magnussen and CLE models

After these first preliminary computations we choose the CLE model, which seems to give more representative results, to continue the analysis. Figure 7 shows the temperature field for three droplet sizes : the nominal value of 82 µm, a lower value (50 µm) and a higher value (115 µm). The three flames are similar in shape with a cold region at the center, corresponding to cold gaseous oxygen, and a flame zone around. The case with 115 µm injected droplet shows a long flame which expands more than the case with 50 µm for instance.

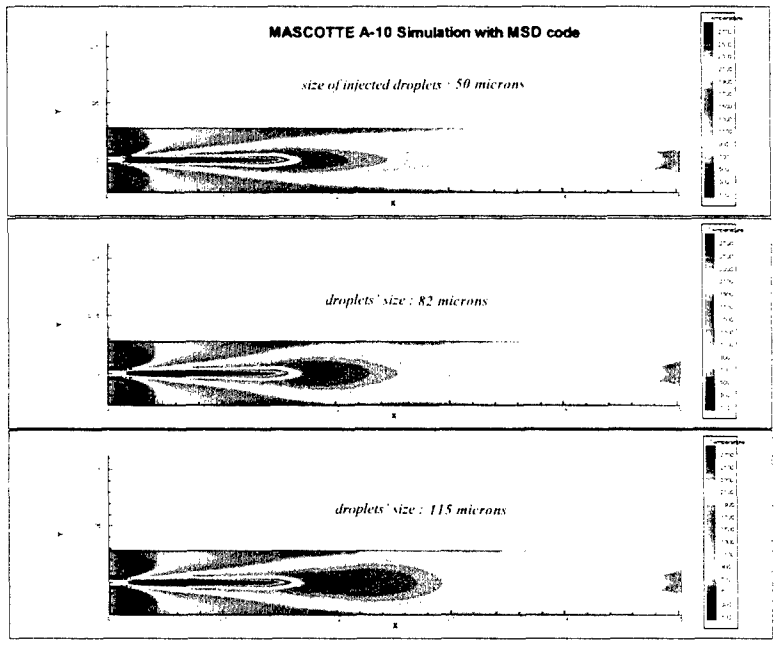

Figure 7 : Temperature field - Effect of droplet size diameter

The corresponding liquid presence and mixture ratio are displayed in figure 8. The figure shows (left) that big drops (82 µm and 115 µm) have crossed the flame.

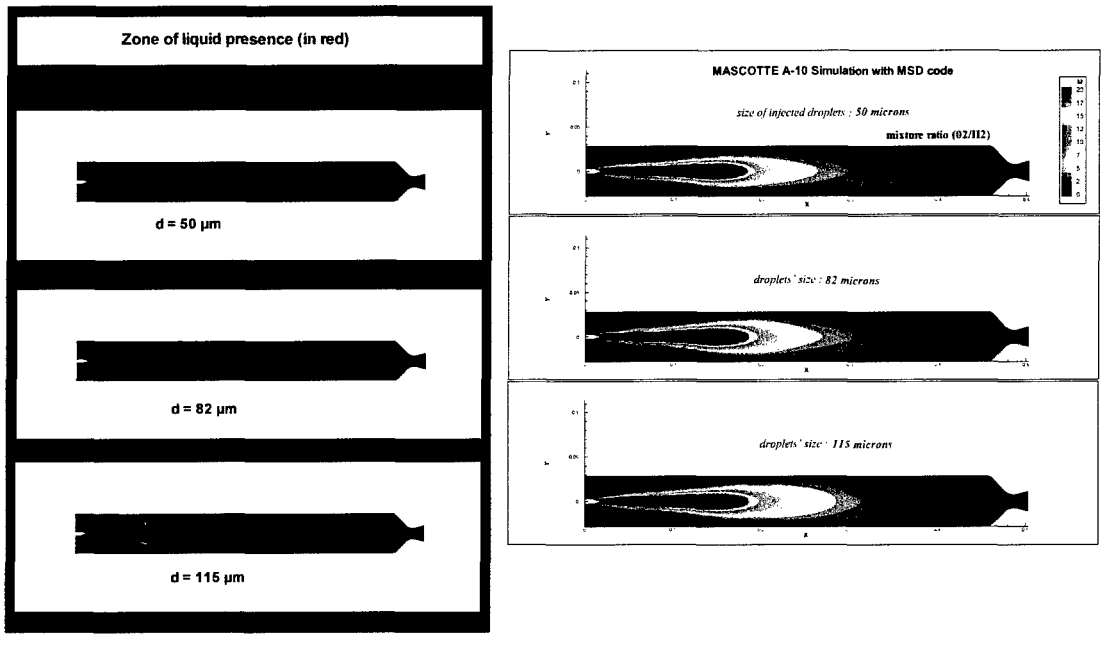

Figure 8 : Liquid presence and mixture ration (O_2/H_2) - Effect of droplet size diameter

Results presented in the subsequent figures correspond to the 82 µm droplets. Figure 9 shows the temperature field and streamlines where the recirculation zone can be observed. Figure 10 shows hydrogen and gaseous oxygen mass fractions.

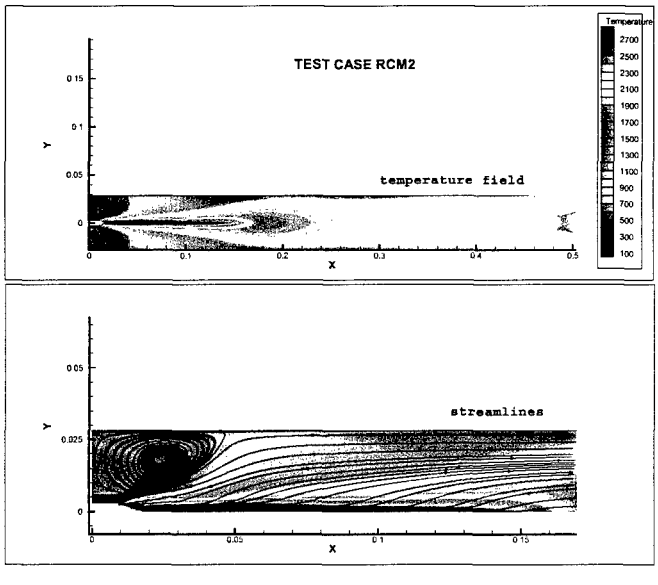

Figure 9 : Temperature field and streamlines - CLE model, D = 82 µm.

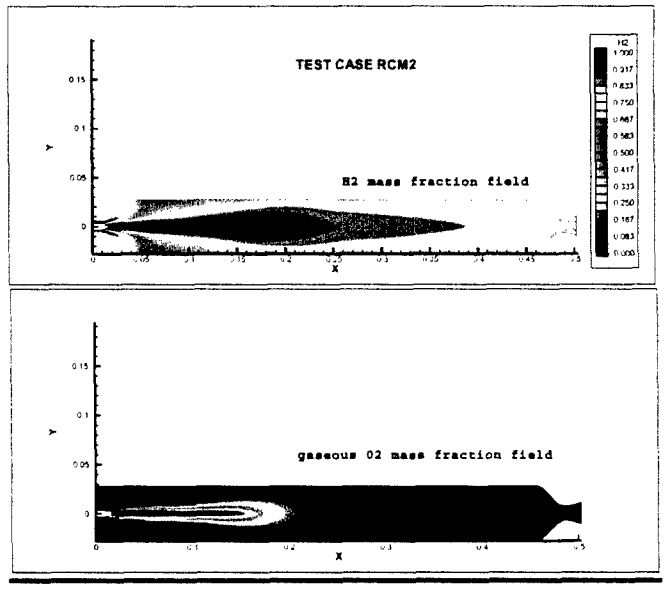

Figure 10 : Mass fractions - CLE model, D = 82 µm.

Figure 11 shows velocity vectors, gas axial velocity, oxygen mass fraction, and hydrogen mass fraction in the near-injector region. One can notice particularly the high hydrogen axial velocity in the injection zone.

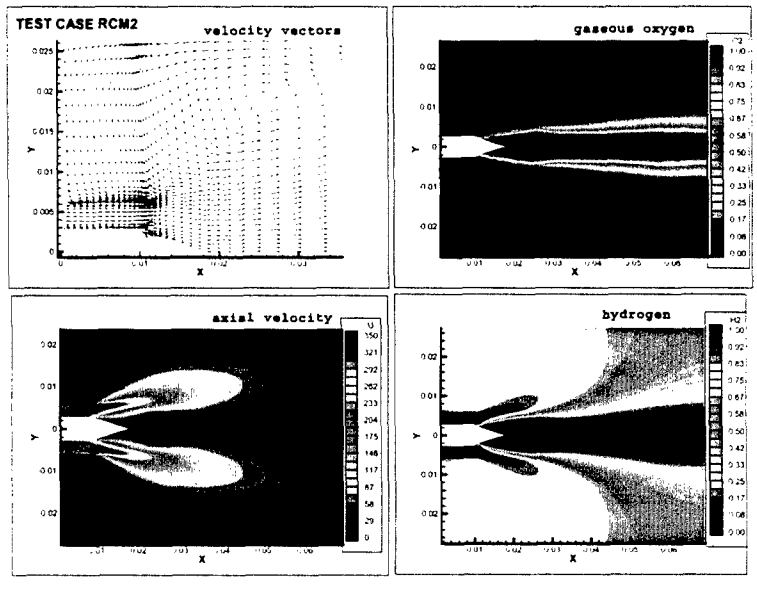

Figure 11 : Velocities and mass fractions in the near-injector zone - CLE model, D = 82 µm.

Figures 12 and 14 show a comparison of computed temperature profiles with experimental data obtained by means of the CARS technique. The CARS technique, using in this case hydrogen as a probe molecule, allows to measure instantaneous gas temperature at a given spatial location. The number on the experimental data (Figures 12 and 14) represents the validation rate which is the ratio of the number of CARS signals successfully processed to the total number of laser shots acquired during a Mascotte run. Nearly 100 laser shots are acquired during a run. At a fixed location, each CARS signal gives an instantaneous temperature. From the instantaneous values one can obtain a mean value and a standard deviation. Of course precision of the measurements depends on the validation rate, higher is this number, better are the statistics. The interval that bounds the experimental data (Figures 12 and 14) represents the standard deviation. The high values of the standard deviation indicate the turbulent character of the flow field.

Figure 12 compares temperature radial profiles at four axial locations : 10, 180, 250, and 410 mm from the injector exit. At 10 mm, one can observe a good agreement between computed results and experimental data.

This region corresponds to the recirculation zone with high concentration of hydrogen which also explains the observed high validation rate. As we move downstream, we have a relatively good agreement with the experimental data. It can be also noticed that the validation rate is low on the axis (x = 180 mm and x = 250 mm) and increases as we move to the chamber wall where more hydrogen in present. No hydrogen is detected on the axis at x = 10 mm.

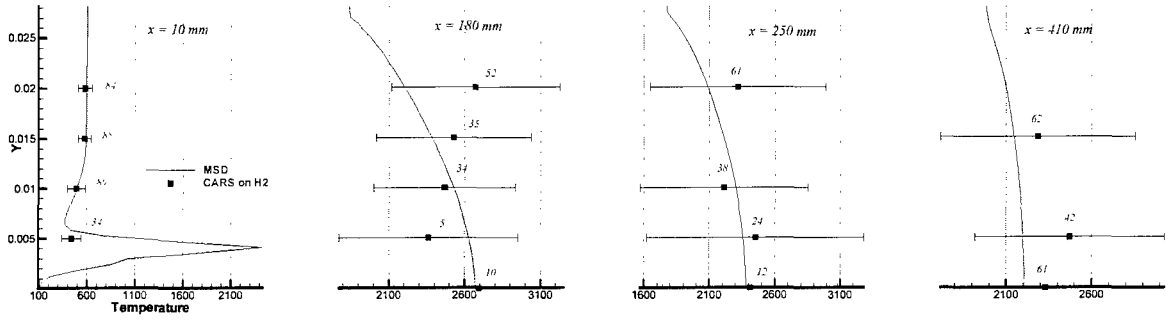

Figure 12 : Temperature radial profiles – Comparison of computations and experimental data

Figures 13 and 14 show temperature axial profiles at three radial locations. (y = 5, 10, and 15 mm). In figure 13, the temperature field is also presented. At 10 and 15 mm, computed profiles are compared with the experimental data. The agreement is fairly good.

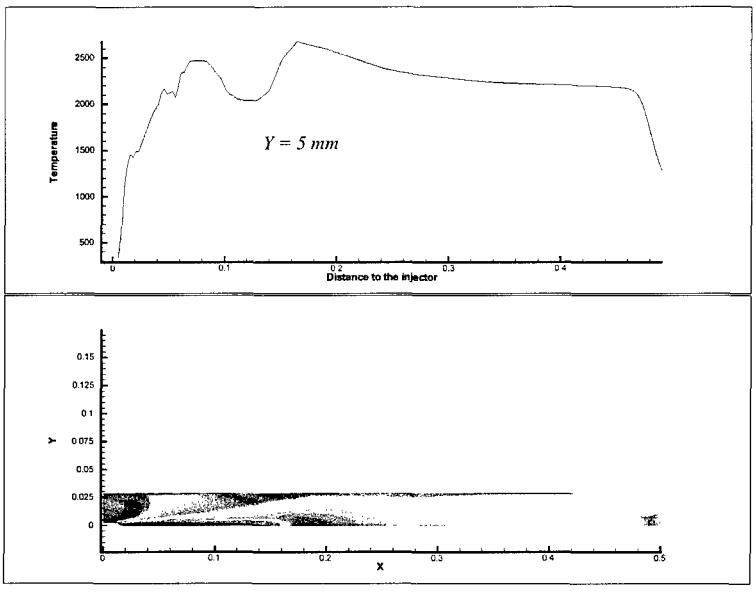

Figure 13 : Temperature field and temperature axial profile at y = 5 mm.

Figures 15 presents temperature radial profiles at other intermediate locations between 10 mm and 410 mm. One can observe that the flame is closed at 200 mm which corresponds to the observed data. At 100 mm, the temperature on the axis seems too low, indicating a poor mixing at this location.

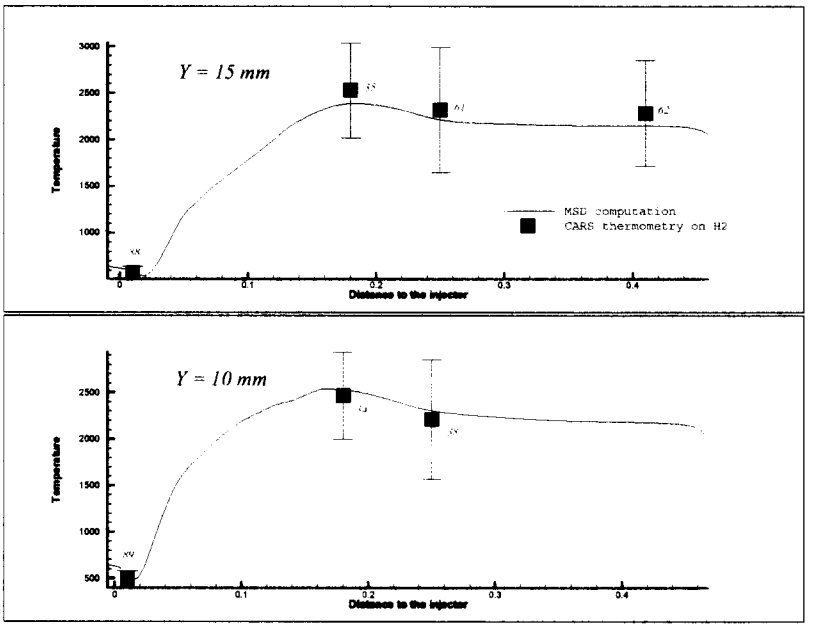

Figure 14 : Temperature axial profiles - Comparison of computations and experimental data (y = 10 mm and y = 15 mm)

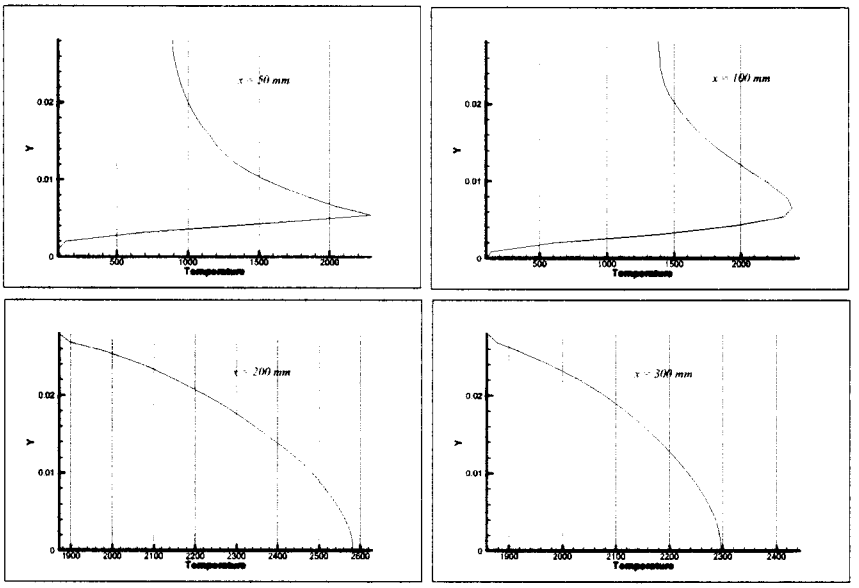

Figure 15 : Temperature radial profiles at other axial locations

7. Conclusion

Numerical simulations of the 10 bar Mascotte flow field performed using the ONERA MSD code have been presented. Droplets were injected along the liquid core represented by a solid cone. Only one class of droplets was injected which diameter was estimated from experimental data. Both kinetic and turbulence models were tested. The turbulent CLE model was found to be the most promising model for these computations. The flame was found to be anchored to the LOX post tip as observed experimentally.

Comparison with CARS data indicate a good agreement in the recirculation zone where temperature is relatively low with high hydrogen concentration. A relatively good agreement is observed on the radial profiles and axial profiles. The flame length could be estimated between 180 and 200 mm.
The flame development could be observed on temperature field and also on intermediate radial profiles of temperature. It seems that the flame does not expand very much compared to the observed data as OH imaging

for instance. Temperature on the axis remains low as far as 100 mm downstream indicating a poor mixing in that region.

Improvements could be searched for by considering a more realistic distribution with more drop sizes, effect of droplets on turbulence level, and other processes such as secondary atomisation and coalescence.

Of course, atomisation is one of the crucial points of this kind of computations as it constitutes the boundary condition for oxygen injection. More representative models have to be developed and used.

References

[1] M. Habiballah, L. Vingert, J.-C. Traineau, P. Vuillermoz, "MASCOTTE : a test bench for cryogenic combustion research", IAF-96-S.2.03, *47th International Astronautical Congress*, (Beijing, China), October 7-10, 1996.

[2] L. Vingert, M. Habiballah, J.-C. Traineau, , "MASCOTTE : a research facility for high pressure combustion of cryogenic propellants", 12th European Aerospace Conference, 3rd European Conference on Space Transportation Systems; November 29 – December 01, 1999, Paris.

[3] L. Vingert, M. Habiballah, P. Vuillermoz, S. Zurbach, "MASCOTTE, a test facility for cryogenic combustion research at high pressure", IAF-00-S.3.06, *51th International Astronautical Congress*, (Rio de Janeiro, Brazil), October 2 - 6, 2000.

[4] E. Villermaux, "Mixing and spray formation in coaxial jets", *Journal of Propulsion and Power*, Vol. 14, n°5, pp. 807-817, Sept-Oct. 1998.

[5] Care, " Etude d'un injecteur coaxial assisté. ", PhD Thesis, Université de Rouen, Décembre 1990.

[6] D. Bissière, " Modélisation du comportement de la phase liquide dans les chambres de combustion de statoréacteurs. ", PhD Thesis, Ecole Centrale, 1997.

[7] G. Turpin, " Revue des modèles de combustion turbulente. Travaux de la 1ère année de thèse. ", Rapport Technique ONERA RT/2/6181 DSNA/Y, Mars 2000.